DEVELOPING AND EXPLOITING A UNIQUE DATASET FROM SOUTH AFRICAN GOLD MINES FOR SOURCE CHARACTERIZATION AND WAVE PROPAGATION

Jordi Julià[1], Andrew A. Nyblade[1], Rengin Gök[2], William R. Walter[2], Lindsay Linzer[3], and Ray Durrheim[3]

Penn State University[1], Lawrence Livermore National Laboratory[2], and
Council for Scientific and Industrial Research[3]

Sponsored by National Nuclear Security Administration

Award Nos. DE-FC52-06NA27320[1] and DE-AC52-07NA27344[2]
Proposal No. BAA06-06

ABSTRACT

In this project, we have developed and exploited a unique seismic dataset to address the characteristics of small seismic events and the associated seismic signals observed at local (< 200 km) and regional (< 2000 km) distances. The dataset has been developed using mining-induced events from three deep gold mines in South Africa recorded on in-mine networks (< 1 km) composed of tens of high-frequency sensors, a network of four broadband stations installed as part of this project at the surface around the mines (1–10 km), and a network of existing broadband seismic stations at local/regional distances (50–1000 km) from the mines. The final dataset includes (i) ~2 years (2007 and 2008) of continuous recording by the surface broadband array and (ii) tens of thousands of mine tremors in the $-3.4 < M_L < 4.4$ local magnitude range recorded by high-frequency in-mine geophones. Events with positive magnitudes are generally well recorded by the surface-mine stations, while magnitudes of 3.0 and larger are seen at regional distances (up to ~600 km) in high-pass filtered recordings.

Significant effort has been devoted to quality control of the in-mine, high-frequency data gathered during this effort. The quality control consisted of (i) identification and analysis of outliers among the P- and S-wave travel-time picks reported by the in-mine network operator and (ii) verification of sensor orientations. The outliers have been identified through a "Wadati filter" developed during this project that searches for the largest subset of P- and S-wave travel-time picks consistent with a medium of uniform wave-speed. We have also detected that trigger times were mistakenly reported as origin times by the in-mine network operator, and corrections have been obtained from the intercept times in the Wadati diagrams. Sensor orientations have been verified by correlating empirically and theoretically rotated P-, SV-, and SH- waveforms. When possible, corrections have been produced through rotations around the vertical components.

Source mechanisms have been investigated by computing full moment tensor solutions for selected events with moment magnitudes in the $0.5 < Mw < 2.6$ range, within the Savuka network volume. The solutions were obtained by inverting P-, SV-, and SH-spectral amplitudes measured on the theoretically rotated waveforms with visually assigned polarities. Most of the solutions revealed the in-mine tremors have a non-zero implosive component (47 out of 76), while a small percentage is purely deviatoric (10 out of 76). The deviatoric component of the moment tensors ranges from pure double couple to pure nondouble couple mechanisms.

Moment tensor solutions and source locations have also been computed for large-magnitude events ($M_L > 3.0$) that were simultaneously recorded by the three in-mine networks and the surface-mine array. During 2007 the high-frequency recordings at one of the mines appeared not to be synchronized with those recorded by the other two mines, so we concentrated our analysis on year 2008. The jointly constrained moment tensor solutions are also dominated by near-vertical, compressional stresses and are more robust than those obtained from the individual in-mine or surface-mine networks. These events are well recorded by AfricaArray stations at local and regional distances.

We have also calibrated the regional stations for seismic coda-derived source spectra and moment magnitude using the envelope methodology of Mayeda (2003). We tie the coda Mw to independent values from waveform modeling. The resulting coda-based source spectra of shallow mining-related events show significant spectral peaking that is not seen in deeper tectonic earthquakes. This coda peaking may be an independent method of identifying shallow events and is similar to coda peaking previously observed for Nevada explosions, where the frequency of the observed spectral peak correlates with the depth of burial (Murphy et al., 2009).

OBJECTIVES

The main objective of this project is to develop and exploit a unique seismic dataset from mine-related events recorded at in-mine (< 3 km), local (3–10 km), and regional (>100 km) distances (Figure 1). The in-mine recordings have been obtained through three in-mine seismic networks consisting of a few tens of high-frequency geophones, which are routinely used to monitor seismic activity in the mines. The local recordings have been acquired through four broadband seismic stations (three Guralp CMG-3T and one Guralp CMG-40T feeding 24-bit RefTek data loggers) deployed under this project and located on the surface of the mining area. And the regional recordings have been acquired mostly through the AfricaArray stations in South Africa and surrounding countries. The dataset that we are assembling is unique in that it contains (1) events spanning several orders of magnitude, (2) events from a range of source depths, and (3) events from a variety of source types (e.g., pillar collapses, tensile fractures, normal and strike-slip faulting, and sources with a significant volumetric component).

We planned to exploit this dataset by using the mining events in 10 related areas of research aimed at improving U.S. operational capabilities to monitor for low-yield nuclear tests: (1) create an event catalog with accurate origin times and locations; (2) determine seismic moment, radiated energy, corner frequency, and stress drop; (3) obtain focal mechanisms from moment tensor inversion; (4) define several categories of event types (shear slip, tensile failure with volumetric component, explosions, pillar collapse) using focal mechanisms and in-mine observations; (5) define and calibrate a coda Mw scale for southern Africa; (6) using calibrated coda techniques, determine Mw for all cataloged events; (7) investigate the effects of depth and source mechanism on the coda-derived source spectra and evaluate the potential of using coda spectral peaking as a depth discriminant; (8) define and calibrate local-to-regional phase (direct P and S, Pn, Pg, Sn, and Lg) propagation characteristics, including the use of the MDAC technique to determine appropriate geometrical spreading and frequency-dependent Q values for the region; (9) characterize relative P and S excitation and source apparent stress resulting from variations in source parameters, including magnitude, mechanism, depth, rock characteristics, and source type; (10) define regional phase ratios that can discriminate between the different source categories, and compare these discriminants and their performance with ongoing work done for other types of mining events, such as in Scandinavia and the western U.S.

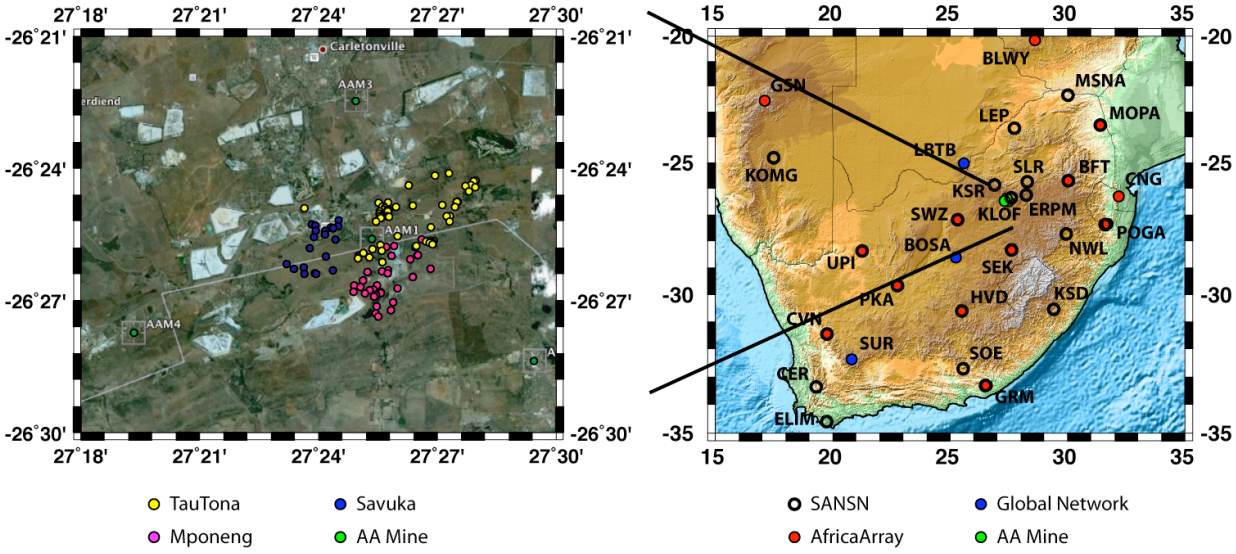

Figure 1. (left) Satellite image from Google Earth showing the Carletonville mining area where the three mines contributing to this project are located. The blue, magenta, and yellow dots are the surface projection of the Savuka, Mponeng, and TauTona in-mine networks, respectively, while the green dots are the surface broadband stations deployed under this effort. (right) Map of broadband stations in South Africa. The red dots are the AfricaArray stations, which are shared with the South Africa National Seismic Network (SANSN) shown as hollow circles, and the blue dots are the three permanent Global Seismographic Network (GSN) stations.

RESEARCH ACCOMPLISHED

A unique dataset of mine-related seismicity to improve U.S. operational capabilities to monitor for low-yield nuclear tests has been developed during this project. The dataset is unique in that it contains events spanning several orders of magnitude ($-3.4 < M_L < 4.4$), recorded at a wide range of epicentral distances, and generated from a variety of source types (mine blasts, pillar collapses, stress fracturing, and faulting events). The collected dataset consists of (i) tens of thousands of high-frequency recordings at near-source distances (< 3 km) from three in-mine networks, (ii) broadband recordings of larger events ($M_L > 1.0$) at local distances (3–10 km) from a surface network in and around the mines, and (iii) broadband recordings of the largest ($M_L > 3.0$) events at near- and far-regional distances (> 200 km) from AfricaArray and Global Seismographic Network (GSN) stations.

The collected dataset has been analyzed to develop (i) event catalogs with accurate event locations (GT1) and origin times, (ii) full moment tensor solutions from spectral amplitudes, and (iii) regional coda-magnitudes and spectra for selected events.

Event Catalogs

Event catalogs for 2007 and 2008 for each mine have been compiled from source locations and local magnitudes provided by the in-mine network operator Integrated Seismic Systems International (ISSI). Locations and origin times were obtained by ISSI from hand picked P- and S-wave arrival times through a ray-tracing algorithm and reported in the local mine-coordinate system and South African local time. We have rebuilt the catalogs to report origin times in Universal Time (UT), epicentral locations in geodetic coordinates (latitude and longitude), and source depths with respect to average mean sea level (a.m.s.l.).

We discovered that the origin times reported by ISSI were actually not origin times but trigger times used to label the events (more precisely, the trigger time corresponding to the first station recording a given event). We were able to obtain origin times from the intercept time in S-P *vs* P travel-time plots (Wadati diagrams) constructed with the hand-picked P- and S-wave travel times provided by ISSI. The accuracy of the origin times was verified during visit to the ISSI branch in TauTona mine in 2008.

Event locations are provided with an accuracy of ~50 m, according to ISSI. Nonetheless, we assessed the hypocentral locations through a simple Geiger inversion of the absolute travel-time picks provided by the in-mine network operator. As we assumed a uniform velocity for the propagating medium, we identified and removed outliers through a "Wadati filter" (Julià et al., 2009a). The "Wadati filter" is a simple search in the (S-P, P) travel-time space that finds the largest subset of (S-P, P) travel-time pairs that follow a straight line (Figure 2), and successfully identifies defective travel-time picks, as well as travel times associated with inhomogeneous ray paths (Julià et al., 2009a). The relocated hypocenters for trial P-wave velocities of 5.8, 5.9, and 6.0 km/s (and

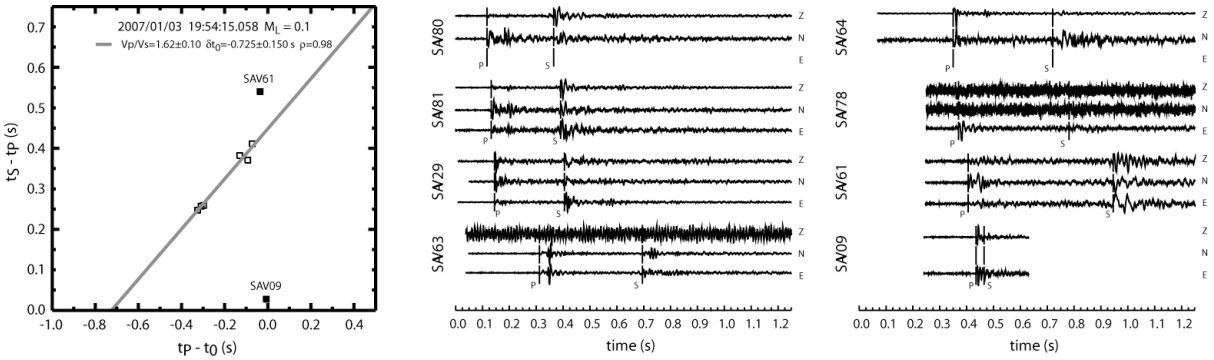

Figure 2. (left) Wadati diagram for a $M_L = 0.4$ event recorded at Savuka mine, South Africa. The solid squares are measurements rejected by the "Wadati filter." The time at the top is a trigger time randomly selected by ISSI to label the event, and used as a reference time in the diagram. (center and right) Recordings for the same events, sorted by P-wave travel time. Note that the waveforms have been normalized to their maximum amplitude. Stations SAV80, SAV63, SAV64, SAV78, and SAV09 have failing channels.

corresponding S-wave velocities computed from a Vp/Vs ratio of 1.64, from the Wadati diagrams) migrated less than 150 m with respect to the original ISSI locations for 50% of the catalog. The origin time corrections obtained from the relocation exercise also correlate well with those obtained from the intercept times in the Wadati diagrams (Figure 3).

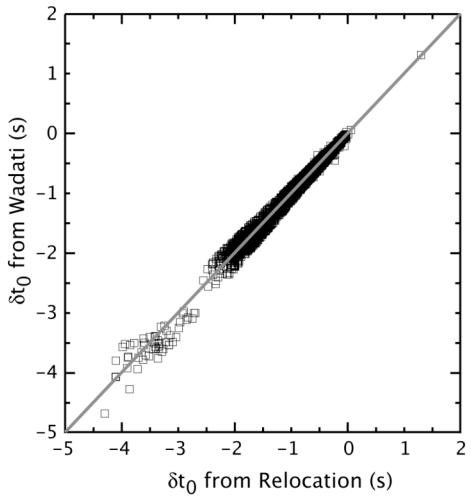

Figure 3. Origin time corrections from the "Wadati filter" vs origin-time corrections from the Geiger relocation (assuming vp = 6.0 km/s).

Savuka Moment Tensor Solutions

We have obtained full moment tensor solutions for 76 events with moment magnitudes between 0.5 and 2.5 by inverting P, SV, and SH spectral amplitudes with polarity attached, as measured on mine tremors recorded by the Savuka in-mine network. We assumed a medium of uniform velocity and density (V_P = 6.0 km/s, V_S = 3.70 km/s, ρ = 2.69 g/cm^3), so the displacements could be expressed as (e.g., Udías, 2000):

$$u_i = G_{ij,k} m_{jk} \quad i,j,k = 1,2,3 \ ,$$

where

$$G_{ij,k} = (1/4\pi\rho v^3 R)\, \gamma_i\gamma_j\gamma_k\, \delta'(t-R/v) \quad \gamma_I = x_i/R$$

and where ρ is density, v is the P- or S-wave velocity, and R is the hypocentral distance. The forward problem was then written by rotating the displacements into the ray-coordinate system and Fourier transforming the resulting equation to obtain spectral amplitudes. This defines a linear problem that was inverted by calculating the natural inverse through a singular value decomposition of the forward problem's matrix (e.g., Menke, 1989).

Spectral amplitudes from the in-mine recordings were obtained through the time-domain procedure of Urbancic et al. (1996). This procedure evaluates the spectral plateau of the P- or S-wave spectrum by computing the ratio

$$\Omega_o = 4(S_{D2})^{3/2}(S_{V2})^{-1/2} \ ,$$

where

$$S_{D2} = 2\int D^2(t)\, dt \quad S_{V2} = 2\int V^2(t)\, dt$$

and D(t) and V(t) are the displacement and velocity, respectively. Following Trifu et al. (2000), the integrals extend between the P- and S-wave travel times, for the P-wave amplitude, and twice the S-P time after the S-wave travel time for the SV and SH amplitudes. The polarity of the spectral amplitudes is assigned visually for each measurement by correlating low-pass filtered waveforms with synthetics.

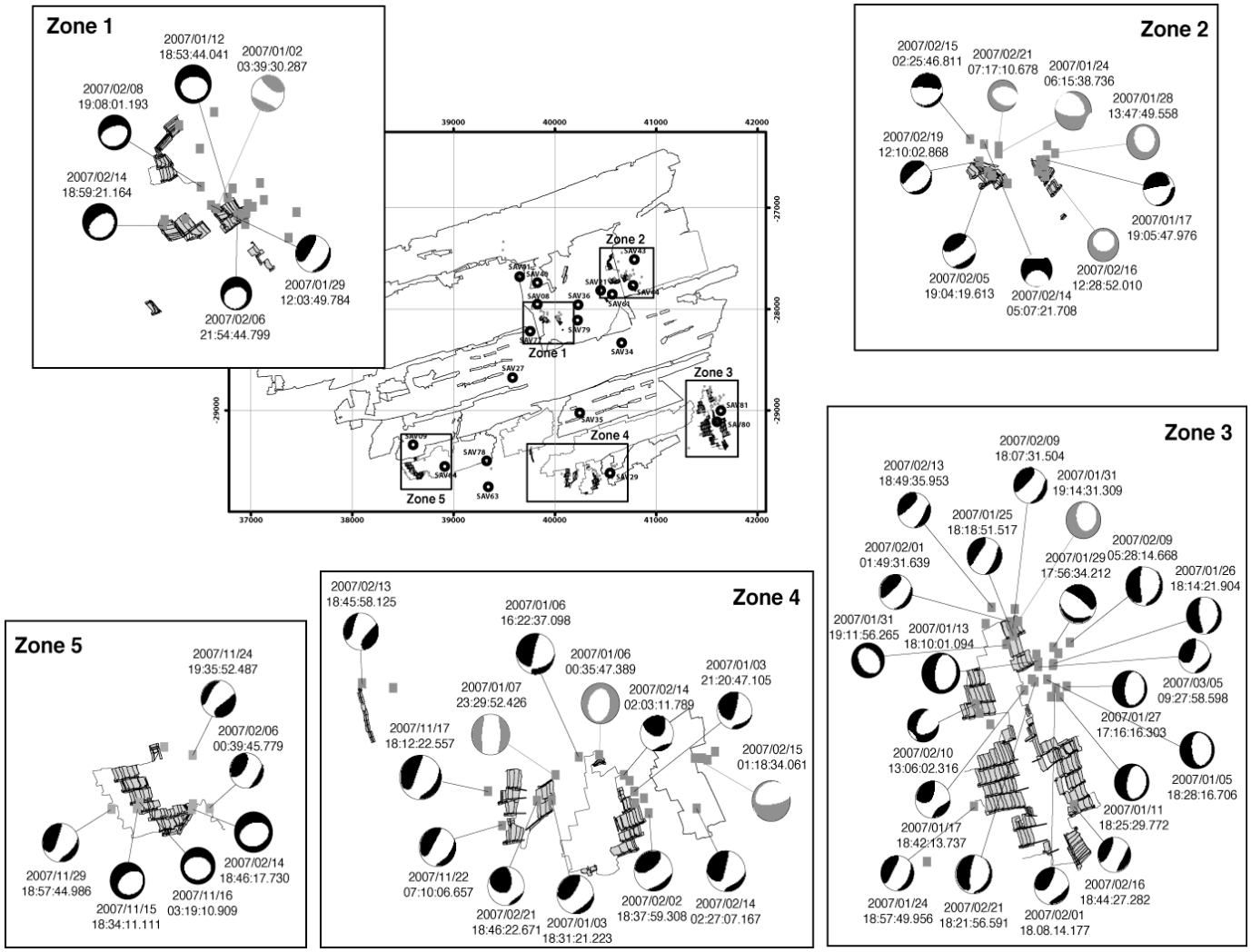

Figure 4. **Spatial distribution of the deviatoric focal mechanisms for the Savuka mine events considered in this study (only those events with a well-constrained deviatoric part have been included). The black symbols represent those events with a significant volumetric component (more than 10% of the total scalar moment); the gray symbols represent those events with a near deviatoric solution (less than 10% of the total scalar moment). The mine plan is the same as in Figure 1, with active areas highlighted.**

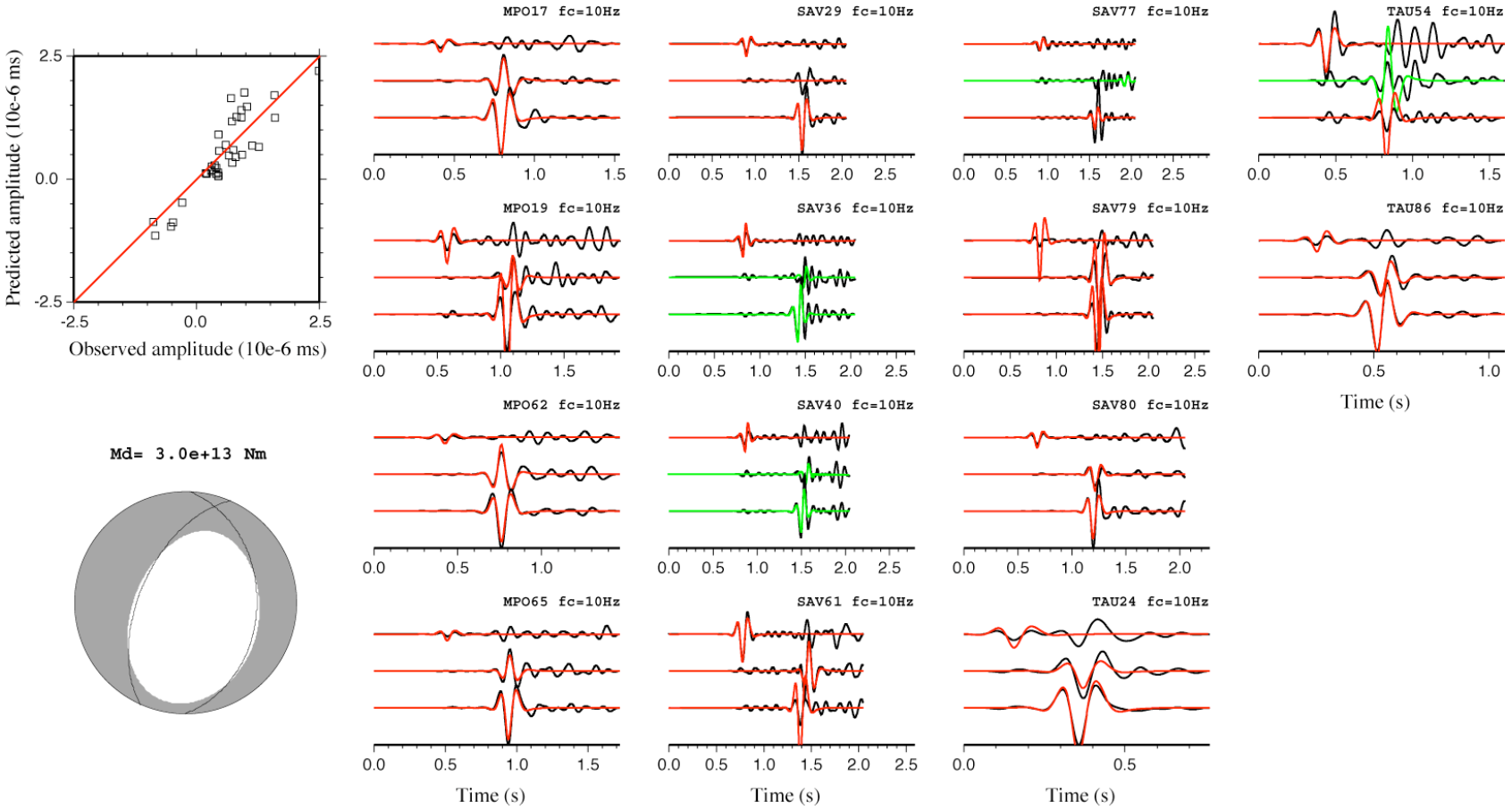

Figure 5. Moment tensor inversion results for a M_L ~3.4 event recorded at the three South African gold mines. The upper left diagram compares predicted and observed spectral amplitudes for P, SV, and SH components. The lower left diagram shows the P-wave radiation pattern for the deviatoric moment tensor. The waveforms on the right are shown to compare the corresponding observed (black) and predicted (red) P, SV and SH amplitudes in the time domain. The green lines are predictions for traces with amplitudes that were not included in the moment tensor inversion. The event origin time is at t = 0 s, and the synthetic waveforms have been shifted to facilitate the comparison with the observations. The time shifts between observed and synthetic waveforms are due to inaccuracies in the event location, assumed wave-speed, and/or anisotropic effects. Note that only spectral amplitudes were inverted, so the observed time shifts did not influence our moment tensor solutions. The waveforms are shown in velocity.

The moment tensor solutions revealed that the largest principal stresses are compressive and oriented near-vertically, consistent with gravity-driven stress conditions in a deep mine and with *in situ* measurements in a nearby deep mine (Pallister et al., 1970). Most of the moment tensor solutions also required a significant implosive component. The robustness of this implosive contribution was assessed by repeating the moment tensor inversion under the additional constraint of a purely deviatoric moment tensor solution, and we found that in 22 occasions the lack of a volumetric component did not degrade the match to the observed spectral amplitudes significantly.

Figure 4 displays the deviatoric "beach-balls" for the 54 events with a well-constrained full moment tensor. The eigenvectors of the deviatoric moment tensor are the same as those for the general moment tensor, so the deviatoric components also have sub-vertical pressure axes and sub-horizontal tension axes. The deviatoric moment tensors can be divided further into two double couples (DCs), consistent with previous works that suggest stresses are relaxed through a combination of co-seismic closure and normal faulting (McGarr, 1992a; 1992b). The deviatoric components can always be decomposed into two DCs, but other decompositions, such as combinations of DC and compensated linear vector dipole (CLVD), are also possible.

The moment tensors for the 76 events recorded by the Savuka in-mine network are reported in Julià et al. (2009b) and can be found online at http://www.geosc.psu.edu/~jjulia/julia-esupp.html.

Joint Inversion of Mine Data

We have selected a total of 43 events with $M_L > 3.5$ (in at least one of the catalogs) that have been well recorded in all the mines in order to determine accurate event locations and moment tensor solutions from the combined dataset. The selection has been performed through sorting and comparison of the event catalogues developed independently for each gold mine for years 2007 and 2008. One of the mines (Mponeng) seems to have had the timing desynchronized with respect to the other mines during 2007, so we are focusing on analyzing events recorded during 2008.

Figure 5 displays a moment tensor inversion from P, SV, and SH spectral amplitudes measured at high-frequency recordings from the three in-mine networks. The eigenvalues are $\sigma_1 = 2.4750 \times 10^{13}$ Nm, $\sigma_2 = 0.4798 \times 10^{13}$ Nm, and $\sigma_3 = -2.9845 \times 10^{13}$ Nm, and the corresponding eigenvectors are $\mathbf{e}_1 = (-0.2475, 0.9524, -0.1778)$, $\mathbf{e}_2 = (0.9420, 0.2795, 0.1856)$, and $\mathbf{e}_3 = (-0.2265, 0.1216, 0.9664)$, which have been constrained to be purely deviatoric. The total scalar moment is $\sim 2.98 \times 10^{13}$ Nm, which corresponds with a moment magnitude around 2.9 (Hanks and Kanamori, 1979). The largest principal stress is compressive ($\sigma_3 < 0$) and subvertical, in good agreement with moment tensor solutions obtained for smaller events at Savuka mine (Julià et al, 2009a; Figure 4). The full moment tensor solution includes a volumetric (implosive) component representing ~17% of the total scalar moment, but it does not improve the match to the observed amplitudes significantly.

Regional Coda Magnitudes and Spectra

We have also been looking at the seismic coda from regional events, both natural earthquakes and mine-related events, that are recorded at regional stations across South Africa. Regional coda envelopes are useful to establish a calibrated moment magnitude scale for the area and to study source spectra of events.

We used the coda wave method of Mayeda (2003) to calculate source spectra of earthquakes recorded at GSN broadband stations and the Kaapvaal seismic array. In order to generate a list of seismic events in the South Africa mining districts, we used the seismic bulletins provided by the Council of Geoscience, Pretoria, and the Preliminary Determination of Epicenters (PDE) catalogs. The mining-induced events were found to be concentrated around Welkom, Klerkdorp, (Far West, West, Central, and East) Rand regions. Tectonic events found in the bulletins primarily consisted of a large Mozambique (Mw = 7.2) event and its aftershocks. The early and late coda parameters were obtained for a set of earthquakes in the region. Those parameters are distance dependent at each narrow frequency band (0.05–6 Hz). The raw amplitudes were path corrected using a Street and Herrmann (ESH) method that corrects for geometrical spreading and Q. The path-corrected amplitudes at 1.0–1.5 Hz are shown in Figure 6.

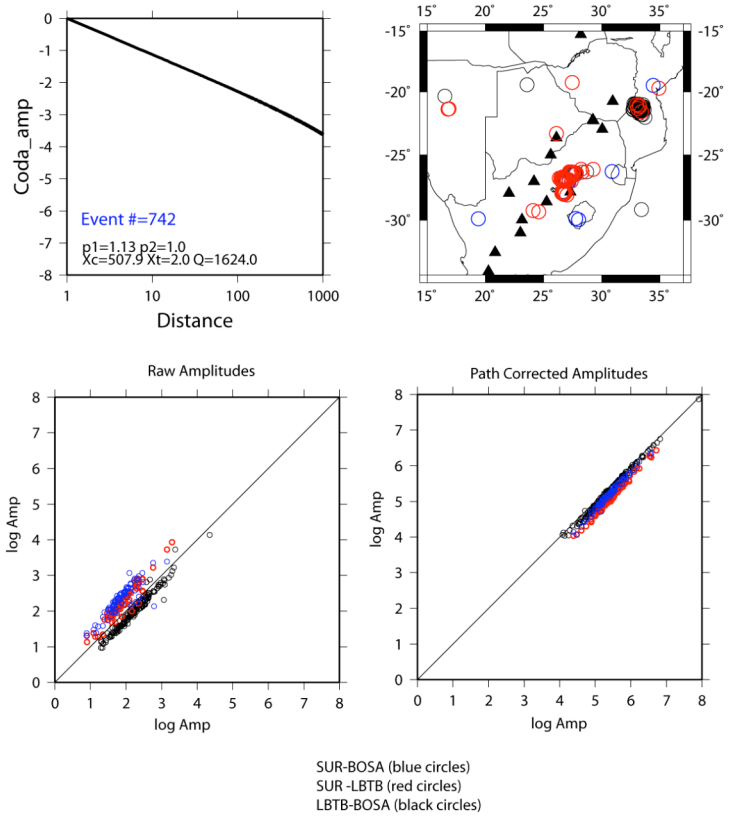

Figure 6. Path calibration at 1.0–1.5 Hz. The upper left panel is the ESH function.

To scale the nondimensional amplitudes to absolute moment, we use independently waveform modeled Mw's. A constant correction factor at each frequency band can then be used to correct for each event to obtain the moment rate function. We performed a grid-search procedure to obtain the body and surface wave fit at long-period levels. The best fitting is obtained at around 1–4 km depth and for a normal fault mechanism. The shallow hypocentral location causes peaking of coda source spectra at 0.4–1.5 Hz. It is probably caused by strong excitation of Rayleigh waves at shallower depth that is then scattered into the coda (Figure 7). The spectral peaking causes overestimated Mw (coda)'s for smaller events where the long period coda levels cannot be measured. Larger-magnitude mining-induced events have coda amplitude values up to a 0.2–0.3 Hz narrow frequency band, where we match the independently waveform-modeled magnitudes. Smaller-magnitude events do not have an amplitude measurement at that frequency. In other words, the coda is abruptly eliminated below 0.2–0.3 Hz for smaller-magnitude events. When we extrapolate the Mw value to the level we expect to measure, then we find an average constant correction factor of 0.4–0.5.

CONCLUSIONS AND RECOMMENDATIONS

We have developed a unique seismic dataset containing events spanning several orders of magnitude ($-3.4 < M_L < 4.4$), recorded at a wide range of epicentral distances and generated from a variety of source types (mine blasts, pillar collapses, stress fracturing, and faulting events). The dataset has been analyzed to determine accurate event locations, full moment tensor solutions, and regional coda magnitudes and spectra. The accuracy of the event locations has been investigated through Geiger-like inversions on select P- and S-wave travel times consistent with a medium of uniform velocity (Julià et al., 2009a), and the moment tensor solutions have been obtained through inversion of P, SV, and SH spectral amplitudes with polarity assigned (Julià et al., 2009b).

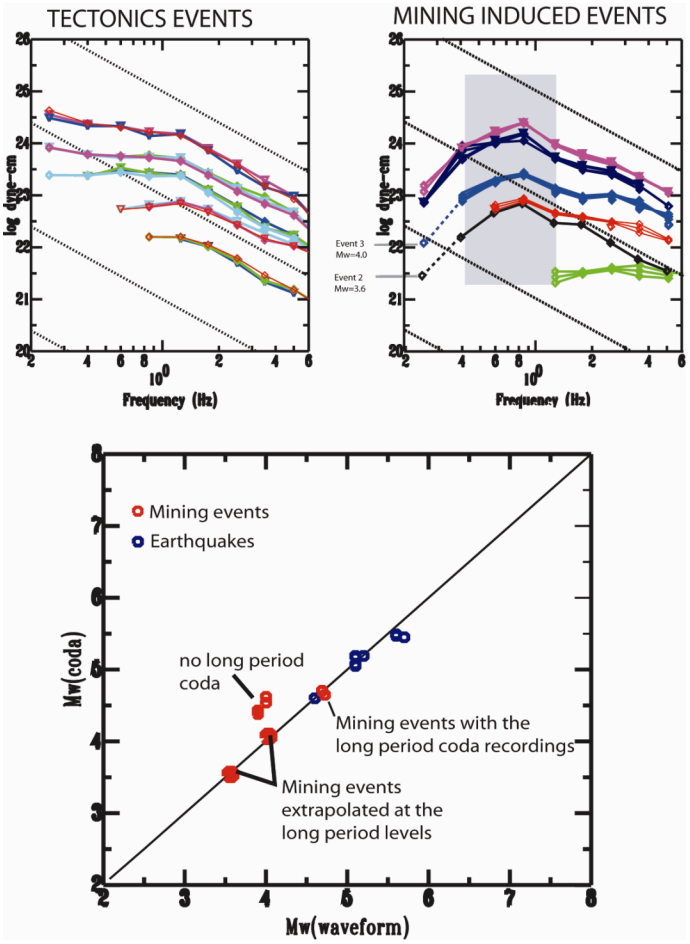

Figure 7. Coda-derived source spectra from earthquakes (left) and mining-induced events (right). The earthquakes have the usual shape: a near constant proportional to the moment at long periods and falling off as frequency^{-2} at the high frequencies. Coda-based Mw's for any event can be determined from the long period level. In contrast, the mine events show an unusual peaked shape, which may be an indicator of shallow depth due to Rg excitation and scattering into the coda. The lowest frequency points shown with dashed lines come from long-period waveform modeling.

We are now constraining moment tensor solutions for large (M_L > 3.5) wells recorded in the three South African mines (Savuka, Mponeng, and TauTona). Preliminary results are consistent with the moment tensor solutions determined for smaller events.

ACKNOWLEDGEMENTS

We thank ISSI and Anglo Gold Ashanti for providing the seismic data and mine plans from the Savuka, Mponeng and TauTona mines. We also thank ISSI and the Council for Scientific and Industrial Research for assisting with event locations and solving other technical issues concerning the in-mine data, and we thank the Council for Geoscience for installing and operating the four broadband stations of the surface mine network. The Data Management Center of the Incorporated Research Institutions (IRIS) for has provided assistance with archiving and distributing data from the permanent AfricaArray seismic stations, including data used in this study.

REFERENCES

Hanks, T. C., and H. Kanamori (1979). A moment magnitude scale, *J. Geophys. Res.* 84: 2348–2350.

Julià, J., A. A. Nyblade, R. J. Durrheim, L. Linzer, R. Gök, W. Walter, S. M. Spottiswoode, and P. Dirks (2009a). A Wadati filter for mine-induced seismicity, *S. Afr. J. Geol.* 112: 371–380.

Julià, J., A. A. Nyblade, R. J. Durrheim, L. Linzer, R. Gök, P. Dirks, and W. Walter (2009b). Source mechanisms of mine-related seismicity, Savuka mine, South Africa, *Bull. Seism. Soc. Am*. 99: 2801–2814.

Mayeda, K. (2003). Stable and transportable regional magnitudes based on coda-derived moment-rate spectra, *Bull. Seism. Soc. Am.* 93: 224–239.

Menke, W. (1989). *Geophysical Data Analysis: Discrete Inverse Theory*. San Diego: Academic Press.

McGarr, A. (1992a). An implosive component in the seismic moment tensor of a mining-induced tremor, *Bull. Seism. Soc. Am.* 19: 1579–1582.

McGarr, A. (1992b). Moment tensors of ten Witwatersrand mine tremors, *Pure Appl. Geophys*. 139: 781–800.

Montalbetti, J. M. and E. R. Kanasewich (1970). Enhancement of teleseismic body waves with a polarization filter, *Geophys. J. R. Astr. Soc.* 21: 119–129.

Murphy, K. R., K. Mayeda, and W. R. Walter (2009), Lg-coda methods applied to Nevada Test Site events: Spectral peaking and yield estimation, *Bull. Seism. Soc. Am.* 99: 441–448.

Pallister, G. F., N. C. Gay, and N. G. W. Cook (1970). Measurements of the virgin state of stress in rock at depth, presented at the 2nd Congress of the International Society for Rock Mechanics, Beograd, 21–26 September 1970.

Trifu, C. I., D. Angus, and V. Shumila (2000). A fast evaluation of the seismic moment tensor for induced seismicity, *Bull. Seism. Soc. Am.* 90: 1521–1527.

Udías, A. (2000). *Principles of Seismology*. Cambridge, UK: Cambridge University Press.

Urbancic, T. I., C. I. Trifu, R. A. Mercer, A.J . Feustel, and J. A. G. Alexander (1996). Automatic time-domain calculation of source parameters for the analysis of induced seismicity, *Bull. Seism. Soc. Am*. 5: 1627–1633.